DOI: 10.3901/CJME.2016.0303.024, available online at www.springerlink.com; www.cjmenet.com

Design and Implementation of a System for Laser Assisted Milling of Advanced Materials

WU Xuefeng*, FENG Gaocheng, and LIU Xianli

School of Mechanical and Power Engineering, Harbin University of Science and Technology, Harbin 150080, China

Received July 29, 2015; revised February 16; accepted March 3, 2016

Abstract: Laser assisted machining is an effective method to machine advanced materials with the added benefits of longer tool life and increased material removal rates. While extensive studies have investigated the machining properties for laser assisted milling(LAML), few attempts have been made to extend LAML to machining parts with complex geometric features. A methodology for continuous path machining for LAML is developed by integration of a rotary and movable table into an ordinary milling machine with a laser beam system. The machining strategy and processing path are investigated to determine alignment of the machining path with the laser spot. In order to keep the material removal temperatures above the softening temperature of silicon nitride, the transformation is coordinated and the temperature interpolated, establishing a transient thermal model. The temperatures of the laser center and cutting zone are also carefully controlled to achieve optimal machining results and avoid thermal damage. These experiments indicate that the system results in no surface damage as well as good surface roughness, validating the application of this machining strategy and thermal model in the development of a new LAML system for continuous path processing of silicon nitride. The proposed approach can be easily applied in LAML system to achieve continuous processing and improve efficiency in laser assisted machining.

Keywords: laser assisted milling, laser assisted milling device, silicon nitride ceramic; finite element analysis, heat transfer

1 Introduction

Advanced high-strength materials such as ceramics and super-alloys have been applied in critical components of aero-engines and gas turbines due to their exceptional mechanical properties(i.e. high-temperature strength, antioxidation properties and corrosion resistance). However, the high cutting forces in these processes usually lead to increased tool wear and low material removal rates which causes inefficiency. Moreover, the need for excessive amounts of cooling lubricants raises not only the processing costs but also the environmental impacts. Laser assisted machining(LAM) is an effective method for machining materials that are typically difficult to machine. LAM uses a high power laser to focally heat a workpiece prior to material removal with a traditional cutting tool. At elevated temperatures, the mechanical properties of the material will change as the yield strength decreases and the material deformation behavior changes from brittle to ductile. This reduces tool wear during the traditional machining process and improves both surface quality and productivity. Use of LAM also eliminates the need for cooling lubricants during dry cutting by using LAM[1–8].

Laser assisted machining includes both laser assisted turning(LAT) and laser assisted milling(LAML). During LAML, a proper cutting tool must be chosen and specific process parameters must be selected due to the intermittent cutting process and the significant impact of laser on the workpiece and cutting tool. Many studies have examined the feasibility and machining performance of LAML. KÖNIG, et al[9], conducted LAML research on stellite, establishing the feasibility of LAML. YANG, et al[10–11], carried out LAML reaction sintered silicon nitride ceramics research, the cutting force and edge crack can effectively reduce by improving the method of controlling cutting temperature. TIAN, et al[12], adopted TiAlN coated carbide tool to LAML studied on Inconel 718, found that when cutting temperature reach at 520 ℃, cutting force reduced by 40%–50%, tool life increased one time and surface roughness reduced to half of its original. BERMINGHAM, et al[13], investigated the wear processes during LAML of hardened stainless steel, observed that tool coating breakdown by abrasive and adhesive wear processes was the dominant mechanism for tool failure and established a simulation method to keep the workpiece heated properly. WIEDENMANN, et al[14], built a FEM simulation model to compute the temperature field from laser radiation. HASSAN, et al[15], established a 3D simulation to optimize

* Corresponding author. E-mail: wuxuefeng@hrbust.edu.cn
Supported by National Natural Science Foundation of China(Grant No. 51205097), and China Postdoctoral Science Foundation(Grant No. 2013M541401)

the process, obtained lower cutting force and tool wear. KIM, et al[16], examined cutting force and preheating temperature prediction for laser assisted milling, prediction equations were developed to calculate the parameters. In addition, the development of laser assisted micro milling(LAMM) has helped to solve problems such as low material removal rates, rapid tool wear failure and poor accuracy of part features through localized thermal softening with the assistance of laser irradiation[17]. MELKOTE, et al[18], developed a LAMM setup capable of producing three dimensional micro-scale features in hard-to-machine materials. These results show good groove dimensional accuracy and low tool wear rates. Other experimental results for LAMM systems in the literature indicate higher material removal rates, reduced tool wear and lower forces[19–21]. However, the milling operation is usually only in one direction, similar to LAML.

Studies on heat conduction, processing mechanism, and processing performance show LAML's ability to improve material processing performance, but it is limited to straight machining, resulting in insufficient processing flexibility and convenience. Conventional methods of LAML position the laser spot on the processing regions in front of the milling cutter transferring heat into the cutting zone through conduction[16]. Such a system is relatively easy to construct by fixing the laser output device on the milling machine. However, ceramic parts with complex geometric shapes and structures cannot be processed using this method because of this fixed position of the laser and cutter. Additionally, thermal energy cannot be used for material plastification in this system and therefore cannot be transferred to the surrounding workpiece. These limitations lead to a very high laser spot center temperatures. BRECHER, et al[22], developed an improved LAML device, where the laser spot was not positioned peripheral to the cutting zone but was projected onto the cutting surface inducing local material plastification before cutting. This approach has the advantage of high heating efficiency by acting directly on the material to be removed leading to energy savings and reduced impact on other areas of the substrate. However, this method is complicated because the laser must be integrated in the machine spindle and synchronized with the cutting edge by discretization and dynamic synchronization. BERMINGHAM, et al[23], proposed two low-cost methods to adapt a commercial CNC milling machine for laser assisted milling, but the device and tests were not implemented.

In this paper, we presented a practical approach for building a laser assisted milling device with improved flexibility and practicality without additional high auxiliary equipment costs. A fixed laser and a rotating machine table are integrated into an existing CNC milling machine to allow LAML while eliminating the need to modify the milling machine. The processing approach, fundamental process investigations, and thermal simulations of the newly designed LAML system are studied and reported below.

2 Technological Concept for Laser Assisted Milling System

The principle of laser assisted machining is represented in Fig. 1. First, the laser irradiates the surface of the workpiece, which is heated by conduction. The increased temperature results in changes in the properties of the material allowing it to be more easily removed by the cutting tool. In conventional machines, the laser spot is focused in front of the surface to be machined as shown in Fig. 1. Before machining, the focusing optical fiber is adjusted to improve the focus of the laser, thus improving the heating of the material. The location of the laser spot cannot be adjusted during machining due to the fixed position of the laser.

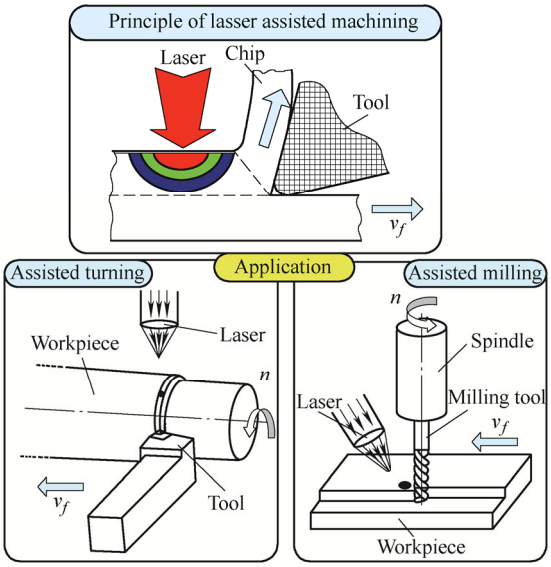

Fig. 1. Schematic of laser assisted machining

In single-direction path machining, the relative position of the milling tool and the laser spot do not need to be changed after laser head adjustment. But for complex path machining, the laser spot does not irradiate the location to be machined once the processing direction changes as shown in Fig. 2. This results in deviating from the processing path for the laser and cooling of the material to be machined. Therefore, for complex path machining, the location of the incident laser must be changed during the machining process in order to continue heating the material.

There are two ways to alter the relative position of the laser spot on the workpiece during processing. The orientation of the incident laser beam can be adjusted, or the direction of the tool path can be changed(Fig. 3(a)). The first approach, the rotating laser solution, requires the laser to move around the milling tool, so a complex optical system or mobile laser head would need to be constructed which would likely lead to equipment interference. This approach is mainly limited due to difficulties in rebuilding

commercial milling machines. The second approach, the rotating table solution, involves altering the relative direction of machining by making the machining path coincide with the laser spot trajectory(Fig. 3(b)). This can be achieved by appending a rotational axis to the device, which alters the relative direction of the tool path.

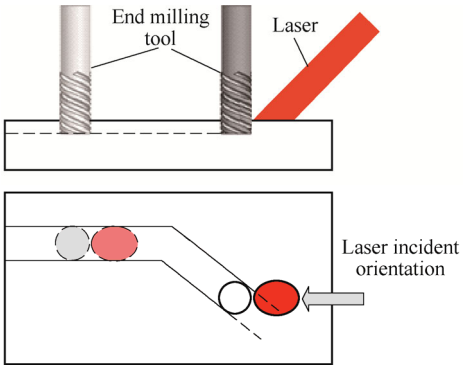

Fig. 2. Relative position of laser beam and milling tool

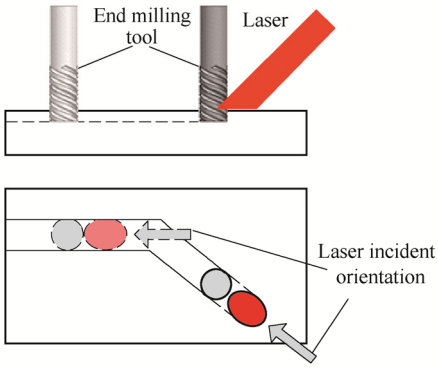

(a) Adjusting the orientation of incident laser

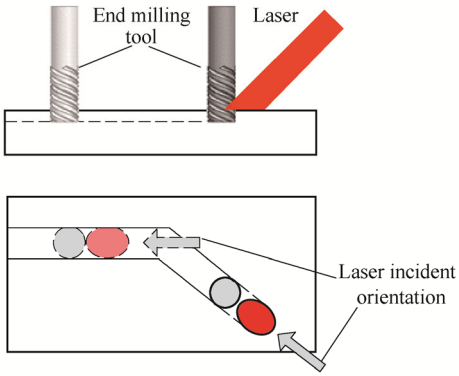

(b) Adjusting the relative direction of machining

Fig. 3. Relative position of laser beam and milling tool

A rotating table can be used to rotate the workpiece by two methods. One method is mount the rotate table on the machine table as shown in Fig. 4(a). The milling tool moves from A to B and the path changes from AB to AB' after the workpiece is rotated around the rotation center. In this scenario the rotation center moves along the process path as shown in Fig. 4(b). The z-axis rises, the milling tool changes position, and the z-axis moves to the original height to continue machining. This method is problematic because it is inefficient and easy to introduce error while the table moves. The second method is to install a 2D-movable worktable on the rotary table(Fig. 4(c)) allowing the rotation center to be concentric with the spindle. Thus the rotating table only changes the relative orientation of the workpiece to the milling cutter leaving the moving table unchanged. In this case, the laser path does not need to be changed, the system is simple and the set-up is convenient. This paper establishes the practicality of this new approach in LAML continuous path systems. Upon the addition of a special rotational worktable, NC processing codes need to be different from convention codes. Because the relative position of the cutting tool and the 2D-moving table do not change while rotating, the three-dimensional movement NC-codes do not need to be modified. The only modification needed is to add the rotation axis to the NC-codes.

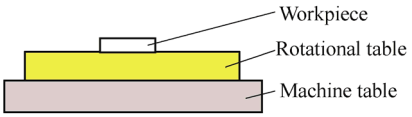

(a) Type of rotation center moves

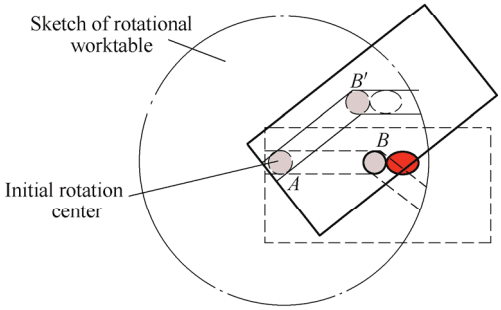

(b) Milling path changes with the workpiece roating

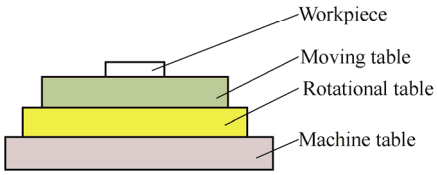

(c) Type of rotation center

Fig. 4. Schematic diagrams of the worktable configuration

A schematic representation of the G-code programming is shown in Fig. 5. OXY is the absolute coordinate system for the milling machine and the processing path follows $A \rightarrow B \rightarrow C$. The path of the laser center relative to the milling tool center is parallel to the x-axis of OXY. When processing to point A, the laser heats along the path $A \rightarrow B$ so the target value of the rotation is θ_1. After processing to point B, the destination of line BC is parallel to the OX-axis. In absolute coordinate terms, the absolute angle value is $-\theta$ and the formula of conversion angle is

$$\theta = \arctan\left(\frac{y_B - y_A}{x_B - x_A}\right), \tag{1}$$

where　θ—Rotation angle of the processing path,
x_A, x_B—Coordinate values of point A and B.

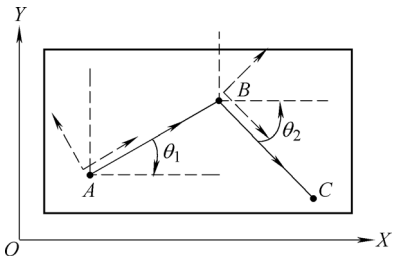

Fig. 5.　Improved schematic diagram for coordinate transformation for LAML

As a result, the value of the computed angle between the x-axis of the coordinate system and the original tool path is the coordinate value of the fourth axis. When machining free curves, straight-line segments are used to approximate the desired path and the rotation angle between the line segments are obtained using the above method. In order to verify the accuracy of the code and the relationship between the laser trajectory and the milling path, VERICUT software is used to simulate the machining process. The model is represented in the Fig. 6. The milling tool is offset by the distance between the laser center and the milling tool center to simulate the trajectory of the laser spot. Therefore, the model can simulate the material removal process of a NC program, optimizing the laser spot position and size.

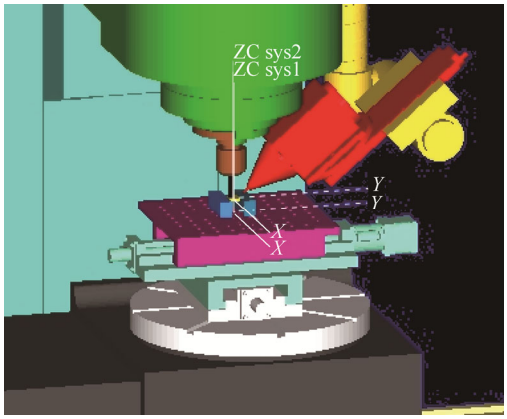

Fig. 6.　VERICUT verification model

Multi-line, free curve machining and laser paths are simulated, the results are shown in Fig. 7. The results indicate that in straight-line machining, the processing path overlaps the laser scan path, but at the turning point the laser spot is outside the machining region while the table rotates. This results from the distance between the laser head and the milling tool. Consequently, the laser power should be reduced or the laser shutter closed when the table rotates to avoid damaging the workpiece. To accomplish this, a laser shutter controlled by the NC system can be used to prevent damage to the workpiece. When machining a free curve, especially when the curvature is small, the paths of the laser and the processing do not completely overlap, so the effect of laser heating on the surface of workpiece should be analyzed. After acquiring the laser path by the VERICUT verification model, the temperature and the stress field can be obtained by finite element simulation in order to help select appropriate process parameters.

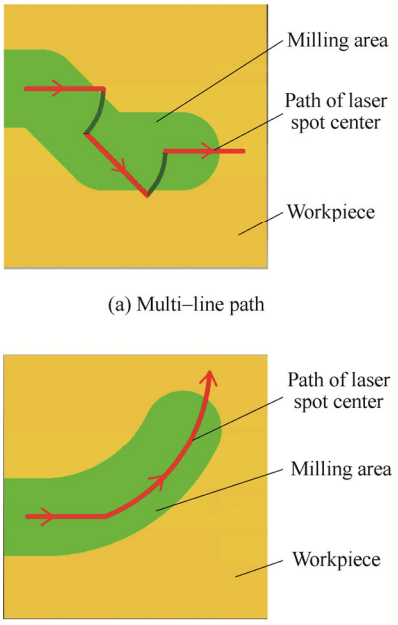

Fig. 7.　Simulated laser scan and machining path for LAML of continuous path

3　Thermal Modeling and Parameters Selection for Laser Assisted Milling

3.1　Thermal modeling for laser assisted milling

In laser assisted machining, maintaining the material removal temperature within a proper range is the most important factor for high quality processing, especially when machining ceramic workpieces. Therefore, thermal analysis should be used to help selecting operating parameters and to provide suggestions for the installation of the system. The thermal model used for temperature distribution in silicon nitride workpiece is based on a 3-D transient heat conduction analysis of a moving Gaussian heat source applied to the workpiece surface. The workpiece in this case is hot-pressing sintering silicon nitride ceramic, with dimensions of 17 mm×17 mm×4 mm. The diameter of cutting tool is 5mm, the rotary table rotation speed is $\pi/4$ rad • s^{-1}. The silicon nitride workpiece is fixed on an insulated table so the bottom surface is considered adiabatic. The boundary conditions include laser heat flux, convection and radiation at the workpiece surface. The convection condition is determined by free convection and radiation exchange between the workpiece surfaces, which is assumed to be a small surface in a large enclosure. At the material removal zone, thermal energy generated by material deformation and tool-workpiece friction is difficult

to model but is assumed to be much less than the energy input from the laser and is neglected in the model[24].

Because the incident laser points obliquely onto the workpiece, the laser spot is elliptical. Therefore, the laser heat flux distribution changes relative to the workpiece after rotating. This was accounted for in the simulation using a coordinate transformation(Fig. 8). When the movement table rotates after the laser spot moves from point A to point B, the coordinate system $X'OY'$ of the model rotates the same amount. The coordinate of point B changes to B' in the new coordinate system $X'OY'$. The transformation formulas of point B' in the new coordinate system after rotation is

$$\begin{cases} x_0' = x_0\cos\theta - y_0\sin\theta, \\ y_0' = x_0\sin\theta + y_0\cos\theta. \end{cases} \tag{2}$$

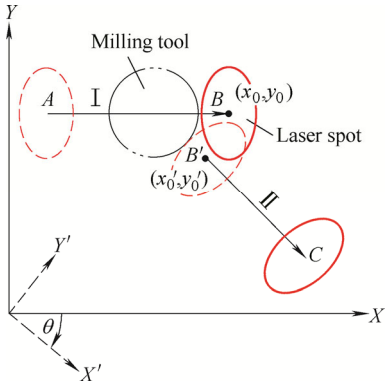

Fig. 8. Coordinate transformation in temperature field modeling

When the transformation is complete, the laser heat flux function does not change. The temperature of the laser spot center(T_{max}) and the farthest point from the cutting area to laser center(T_{min}) is determined as reference temperatures in order to measure the influence of laser heating. Ideally, T_{min} should exceed the temperature at which the material softens(900 ℃) and T_{max} should be below the melting temperature of the material. Because T_{min} and T_{max} may not fall entirely on the node of the finite element model, the node interpolation method was used to obtain accurate temperature values. The interpolation process is shown in Fig. 9, and T_E, the interpolation temperature of point E, is equal to

$$T_E = \frac{1}{4}\left[T_A(1-s)(1+t)+T_B(1+s)(1+t)+ T_C(1-s)(1-t)+T_A(1+s)(1-t)\right], \tag{3}$$

where $s = 2\left(x_E - \dfrac{x_C+x_D}{2}\right)/(x_D-x_C)$,

$t = 2\left(y_E - \dfrac{y_C+y_A}{2}\right)/(y_A-y_C)$.

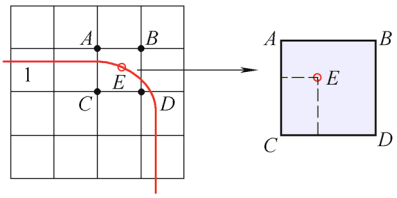

Fig. 9. Schematic of process for temperature interpolation

The model was corrected and verified using a temperature measuring experiment[25]. According to the model, the maximum temperature is under the laser beam with a large temperature gradient around the laser spot due to the low conductivity of silicon nitride. Laser power has the most significant impact on workpiece temperature, so the appropriate laser power needs to be chosen to provide the right amount of energy for material softening. Another important parameter in LAM is the lead distance between the laser beam and the cutting tool. As the lead distance increases, the absorption of energy into the workpiece via conduction increases which causes a significant temperature decrease on the surface. Therefore, the cutting area should be close to the laser spot, but the distance between the two regions needs to be high enough to prevent the tool body from being directly affected by the laser. Our results show that temperature decrease while moving away from the laser spot follows a Gaussian distribution. Therefore, the diameter of the cutter should be limited to a range less than the diameter of the laser beam. The laser beam diameter, which has a significant effect on the temperature gradient, should not be less than 3 mm.

Laser preheating on the edge of the workpiece is used to increase the initial processing temperature and reduce the yield strength of the material. The size of the laser spot should not be too small, or excessive thermal stress could lead to cracks, as shown in Fig. 10. As the performance is limited by the small, two-dimensional testing stage, vibrations caused by the large cutting force result in increased tool wear and edge chipping. Therefore, relative small cutting parameters are used to verify the feasibility of the system. According to the machining parameters characteristics mentioned above, a finite element model was established as shown in Fig. 11 and the machining parameters are outlined in Table 1. Two representative paths, a continuous line and a curved path, were investigated. The procedures for these machining paths are as follows.

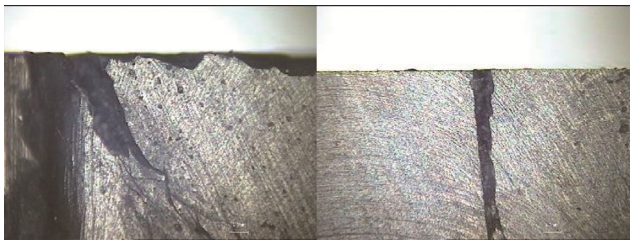

Fig. 10. Cracks of workpiece induced by thermal stress

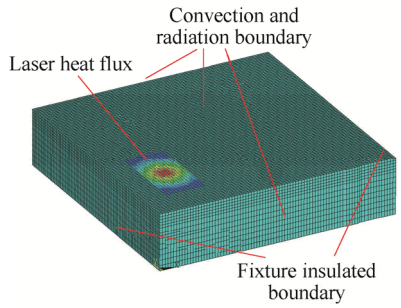

Fig. 11.　Schematic of process for temperature interpolation

Table 1.　Machining parameters of LAML

Machining parameter	Value
Laser power P_l / W	110
Rotate speed n / (r • min^{-1})	590
Feed rate f / (mm • r^{-1})	0.05
Cutting depth a_p / mm	0.2
Laser diameter D_l / mm	4
Preheating time t_p / s	25

3.2　Continuous line path

A typical milling tool and laser heating path are shown in Fig. 12. First, the laser is preheated at point A' before processing and the milling tool started moving after the laser temperature reached the material's softening temperature. The milling tool moves from A to B, followed by a rotation of the laser center point from B' to B'' after which processing continues. After the milling tool reaches point C, the laser center point rotates from C' to C'', and the processing finishes after the milling tool reaches point D. The temperature and stress fields of laser heating obtained by simulation are shown in Fig. 13.

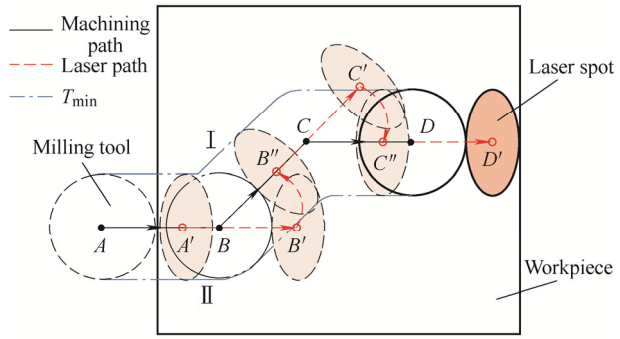

Fig. 12.　Continuous linear cutting and laser heating path

The temperature at the center of the laser spot is about 1300 ℃ and the whole workpiece becomes hot after laser heating due to its small size. Silicon nitride ceramics have good performance at elevated temperatures with working temperatures up to 1200 ℃. This temperature can only be achieved within the laser spot diameter and the ablated material would be removed by milling tool while the un-machined area keeps the material performance. T_{min} and T_{max} vary with time, as shown in Fig. 14. T_{cutI} and T_{cutII} are the temperatures at the machining boundaries. T_{cutI} and T_{cutII} are different because their distance from the edge changes as processing proceeds. Preheating of the laser for 25 s is sufficient to reduce laser temperature fluctuation. As the laser moves toward to the inside of workpiece, heat is conducted over a wide range so T_{max} and T_{cut} gradually decrease. The temperature of the entire workpiece is high and T_{min} is above the softening temperature of 900 ℃.

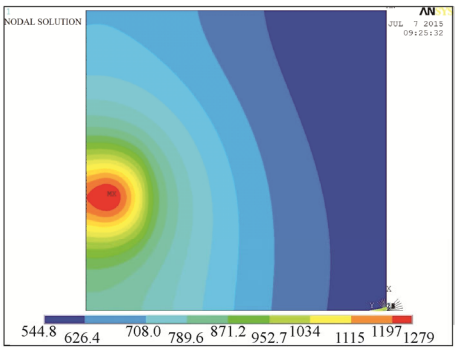

(a) 25 s

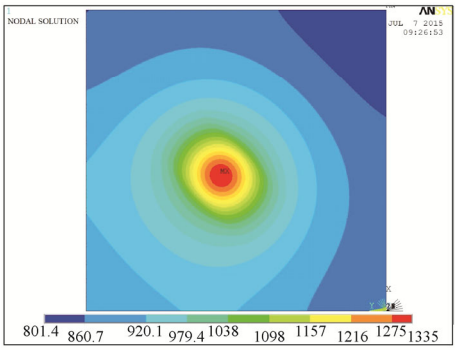

(b) 60 s

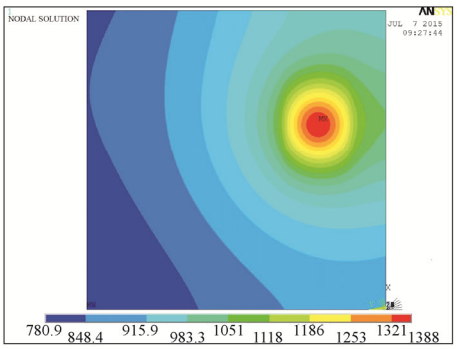

(c) 95 s

Fig. 13.　Temperature fields for line path heating at different times

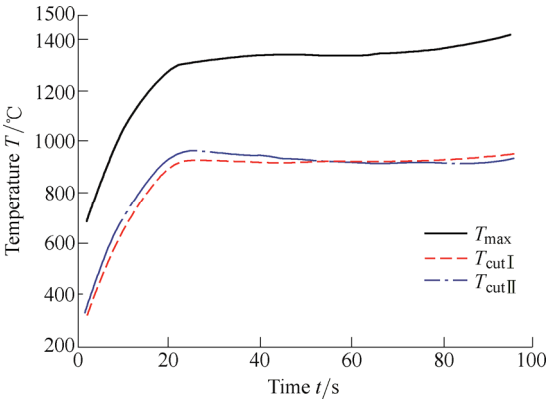

Fig. 14.　Temperature histories for T_{max} and T_{cut}

3.3 Continuous curve path

The continuous curve cutting and laser heating path are shown in Fig. 15. Since the milling tool center is the rotation center, the laser beam and the horizontal position of the milling cutter remain unchanged along the path coordinates. Within this path, the location of the laser spot does not coincide with the milling cutter. The temperature field distribution during laser heating is shown in Fig. 16.

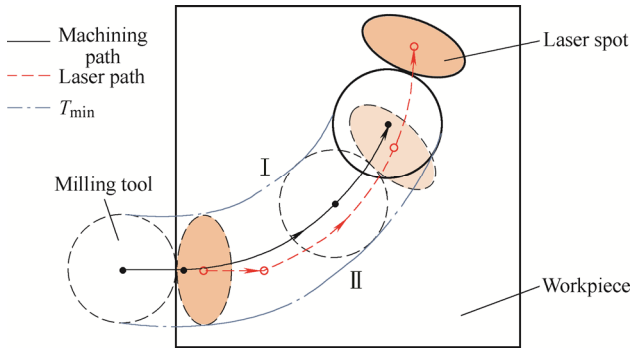

Fig. 15. Continuous curve cutting and laser heating path

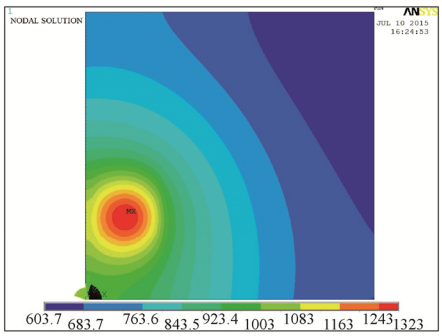

(a) 30 s

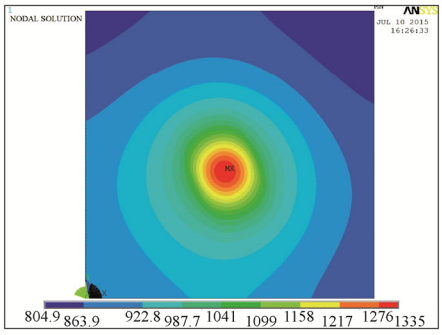

(b) 60s

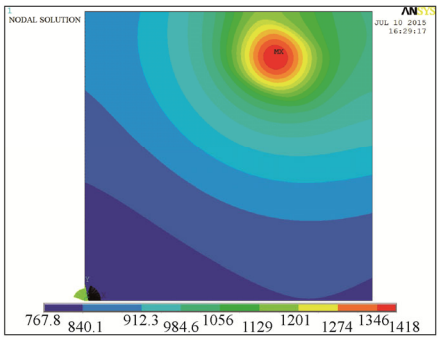

(c) 210s

Fig. 16. Temperature fields for curve path heating at different times

The temperature of the incident laser beam area becomes very high and the workpiece reaches 1420 ℃ due to heat conduction. The relative direction of the laser spot and workpiece changes along the machining path, but T_{max} is mostly unchanged. As the laser spot moves closer to the workpiece boundaries, T_{max} and T_{cut} gradually increase as shown in Fig. 17. The edge of the laser spot is low in energy so the temperature does not exceed the operating temperature of the material. T_{cutI} and T_{cutII} are different because of different distances between the workpiece boundaries as processing proceeds. Both T_{cutI} and T_{cutII} are controlled to be above the softening temperature of 900 ℃ by selecting milling parameters so the softened materials can be removed by milling tool.

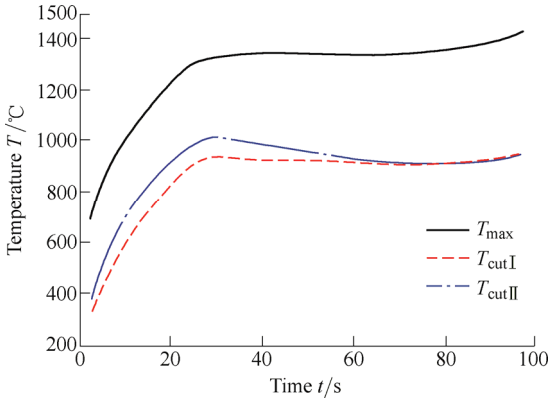

Fig. 17. Temperature histories for T_{max} and T_{cut}

4 System Setup and Experimental Results

Processing and temperature simulations show that the designed system and machining strategies are feasible. An experimental system was set up to validate the design in LAML of silicon nitride. The experimental system was implemented by retrofitting an existing 3-axis CNC milling machine as shown in Fig. 18. A rotary table was fixed on the milling table such that the rotary center was concentric with the spindle. A 2D worktable was then installed on the rotary table so that the rotary table only changed the direction of machining. The 2D worktable and the z-axis of the milling machine make up the 3 axis for milling operation. A 300 W continuous wave Nd: YAG laser was used to generate the laser beam in front of a milling tool. The laser beam was delivered through a fiber optic and focused on the workpiece surface at an angle of about 60°. A laser head fixture that can be used to adjust the relative position between the laser and the workpiece was fixed to the milling head. The diameter of the PCBN end milling tool is 5 mm and can operate at higher temperature than silicon nitride. During milling, the laser beam did not move with the workpiece, instead the worktable rotated to change the relative positions of the moving direction and incident laser beam. Therefore, the relative positions of the laser spot and the cutting edge were unchanged during milling. Control of the laser shutter was integrated into the NC

system to ensure the synchronization of the two subsystems during LAML.

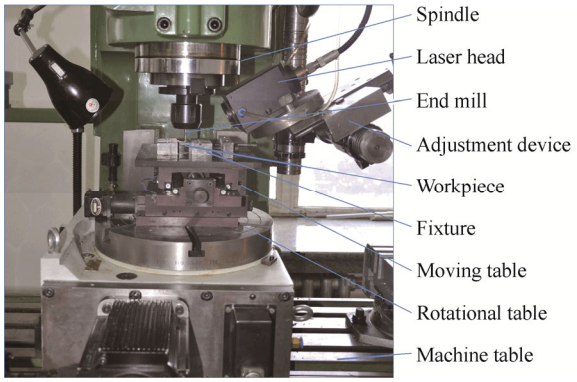

Fig. 18. Improved experimental system for continuous LAML

The machining parameters are the optimized parameters from the simulations, as shown in Table 1. The continuous line and curved machined workpieces are shown in Fig. 19. The surface quality of the machined material is good and there is no significant damage or cracks in the structure.

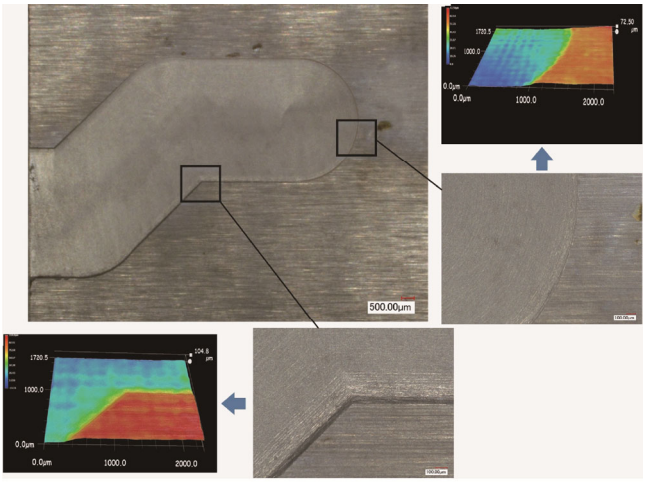

(a) Continuous linear cutting

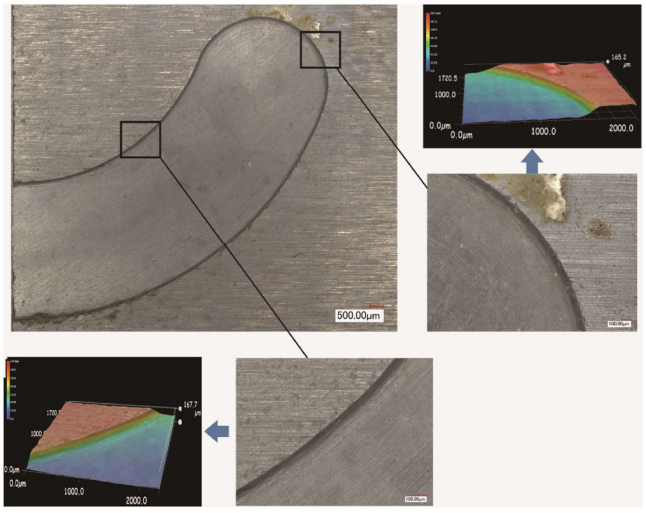

(b) Continuous curve cutting

Fig. 19. Workpiece of continuous path machined by LAML

The average surface roughness(*Ra*) of the machined surfaces were measured by the instrument(PGI 1240 from Taylor Hobson) at three position and the results are 0.2 μm and 0.28 μm, respectively. After processing, some laser irradiated material is not removed by the tool, so there is significant ablation present on the workpiece surface.

The results show that reasonable processing parameters can be selected from a combination of path conversions, NC codes verification, and temperature distribution predictions. Using our new procedure, complex path machining by LAML can be achieved with high machining quality. Therefore, complex ceramic parts can be machined by LAML in an efficient and cost-effective manner. Further process analysis of this device will provide the necessary application and parameter ranges for other materials and machining conditions.

5 Conclusions

(1) An inexpensive and practical laser assisted milling system is designed and established using a rotary table integrated into a 3-axis machine tool and combined with a laser system. The system has the ability to machine complex continuous paths.

(2) Based on the coordinate transformation method, NC-codes for the system are programmed to ensure that the laser always heats the material ahead of the milling cutter. The VERICUT verification model shows that the laser spot is outside of the machining region as the rotating table rotates, therefore the laser heating temperature should be controlled to avoid thermal damage.

(3) A transient thermal model is established for laser assisted milling of continuous line and curved paths. The model can be used to select machining and laser parameters to keep the temperature of the cutting area above the softening temperature of 900 ℃ while machining silicon nitride ceramics.

(4) Continuous paths are successfully machined on the silicon nitride workpiece by an end milling tool with laser heating. The roughness of the machined surfaces is 0.2 μm and 0.28 μm for the straight line and curved path, respectively. There are no apparent cracks on either workpiece. The results prove the machining capacity of the system and the feasibility of machining complex workpieces.

References

[1] MASOOD S H, ARMITAGE K, BRANDT M. An experimental study of laser assisted machining of hard-to-wear white cast iron[J]. *International Journal of Machine Tools and Manufacture*, 2011, 51(6): 450–456.

[2] KIM J D, LEE S J, SUH J. Characteristics of laser assisted machining for silicon nitride ceramic according to machining parameters[J]. *Journal of Mechanical Science and Technology*, 2011, 25(4): 995–1001.

[3] BEJJANI R, SHI B, ATTIA H, et al. Laser assisted turning of Titanium metal matrix composite[J]. *CIRP Annals-Manufacturing Technology*, 2011, 60(1): 61–64.

[4] DING Hongtao, SHIN Y C. Laser-assisted machining of hardened steel parts with surface integrity analysis[J]. *International Journal of Machine Tools and Manufacture*, 2010, 50(1): 106–114.
[5] DANDEKAR C R, SHIN Y C. Laser-assisted machining of a fiber reinforced metal matrix composite[J]. *Journal of Manufacturing Science and Engineering*, 2010, 132(6): 061004.
[6] DANDEKAR C R, SHIN Y C, BARNES J. Machinability improvement of titanium alloy(Ti-6Al-4V) via LAM and hybrid machining[J]. *International Journal of Machine Tools and Manufacture*, 2010, 50(2): 174–182.
[7] ANDERSON M, PATWA R, SHIN Y C. Laser-assisted machining of Inconel 718 with an economic analysis[J]. *International Journal of Machine Tools and Manufacture*, 2006, 46(14): 1879–1891.
[8] SKVARENINA S, SHIN Y C. Laser-assisted machining of compacted graphite iron[J]. *International Journal of Machine Tools and Manufacture*, 2006, 46(1): 7–17.
[9] KÖNIG W, ZABOKLICKI A K. Laser-assisted hot machining of ceramics and composite materials[C]//*Proceedings of the International Conference on Machining of Advanced Materials,* Gaithersburg, USA, July 20–22, 1993. Gaithersburg: NIST, 1993: 455–463.
[10] YANG B, SHEN X, LEI S. Mechanisms of edge chipping in laser-assisted milling of silicon nitride ceramics[J]. *International Journal of Machine Tools and Manufacture*, 2009, 49(3–4): 344–350.
[11] YANG B, LEI S. An experimental study of laser assisted milling of silicon nitride ceramic[C]//*Transactions of the North American Manufacturing Research Institution of SME 2007*, Ann Arbor, USA, May 22–25, 2007. Dearborn: SME, 2007: 473–480.
[12] TIAN Yinggang, WU Benxin, ANDERSON Mark, et al. Laser-assisted milling of silicon nitride ceramics and Inconel 718[J]. *Journal of Manufacturing Science and Engineering*, *Transactions of the ASME*, 2008, 130(3): 0310131–0310139.
[13] BERMINGHAM M J, KENT D, DARGUSCH M S. A new understanding of the wear processes during laser assisted milling 17-4 precipitation hardened stainless steel[J]. *Wear*, 2015, 4(328–329): 518–530.
[14] WIEDENMANN R, ZAEH M F. Laser-assisted milling—Process modeling and experimental validation[J]. *CIRP Journal of Manufacturing Science and Technology*, 2015, 8(1): 70–77.
[15] HASSAN Z, JAN P H, BERNHARD S, et al. 3D simulation and process optimization of laser assisted milling of Ti6Al4V[C]//*14th CIRP Conference on Modeling of Machining Operations, CIRP CMMO 2013*, Turin, Italy, June 13–14, 2013, Amsterdam: Elsevier, 2013: 75–80.
[16] KIM D, LEE C. A study of cutting force and preheating temperature prediction for laser-assisted milling of Inconel 718 and AISI 1045 steel[J]. *International Journal of Heat and Mass Transfer*, 2014, 71: 264–274.
[17] CHENG K, HUO D. *Micro Cutting: Fundamentals and Applications*[M]. Chichester: John Wiley & Sons Ltd, 2013.
[18] MELKOTE S, KUMAR M, HASHIMOTO F, et al. Laser assisted micro-milling of hard-to-machine materials[J]. *CIRP Annals-Manufacturing Technology*, 2009, 58(1): 45–48.
[19] KUMAR M, MELKOTE S N. Process capability study of laser assisted micro milling of a hard-to-machine material[J]. *Journal of Manufacturing Processes*, 2012, 14(1): 41–51.
[20] KUMAR M, MELKOTE S N, SAOUBI R M. Wear behavior of coated tools in laser assisted micro-milling of hardened steel[J]. *Wear*, 2012, 296: 510–518.
[21] DING Hongtao, SHEN Ninggang, SHIN Y C. Thermal and mechanical modeling analysis of laser-assisted micro-milling of difficult-to-machine alloys[J]. *Journal of Materials Processing Technology*, 2012, 212(3): 601–613.
[22] BRECHER C, EMONTS M, ROSEN C J, et al. Laser-assisted Milling of Advanced Materials[C]//*Lasers in Manufacturing 2011-Proceedings of the 6th International WLT Conference on Lasers in Manufacturing*, Munich, Germany, May 23–26, 2011. Amsterdam: Elsevier, 2011: 599–606.
[23] BERMINGHAM M J, SCHAFFARZYK P, PALANISAMY S, et al. Laser-assisted milling strategies with different cutting tool paths[J]. *International Journal of Advanced Manufacturing Technology*, 2014, 74(9–12): 1487–1494.
[24] SHEN X, LEI S. Thermal modeling and experimental investigation for laser assisted milling of silicon nitride ceramics[J]. *Journal of Manufacturing Science and Engineering, Transactions of the ASME*, 2009, 131(5): 0510071–05100710.
[25] WU Xuefeng. *Basic Research on Laser Assisted Machining of Silicon Nitride Ceramics*[D]. Harbin: Harbin Institute of Technology, 2011. (in Chinese)

Biographical notes

WU Xuefeng, born in 1982, is currently an associate professor at *Harbin University of Science and Technology, China*. He received his PhD degree from *Harbin Institute of Technology, China*, in 2011. His research interests include laser assisted machining, cutting technology, cutting database and cloud manufacturing.
Tel: +86-451-86390533; E-mail: wuxuefeng@hrbust.edu.cn

FENG Gaocheng, born in 1991, is currently a master candidate at *Harbin University of Science and Technology, China*. His research interests include metal cutting technology.
Tel: +86-451-86390533; E-mail: 18772728807@163.com

LIU Xianli, born in 1961, is currently a professor at *Harbin University of Science and Technology*, *China*. He received his PhD degree from *Harbin Institute of Technology*, *China*, in 1999. His research interests include metal cutting theory, cutting tool technology and digital processing technology.
Tel: +86-451-86390501; E-mail: xlliu@hrbust.edu.cn